

## Quantitative sampling using an Aerodyne aerosol mass spectrometer

### 2. Measurements of fine particulate chemical composition in two U.K. cities

James D. Allan,<sup>1</sup> M. Rami Alfarra,<sup>2</sup> Keith N. Bower,<sup>1</sup> Paul I. Williams,<sup>1</sup>  
 Martin W. Gallagher,<sup>1</sup> Jose L. Jimenez,<sup>3,4</sup> Alan G. McDonald,<sup>5</sup> Eiko Nemitz,<sup>5</sup>  
 Manjula R. Canagaratna,<sup>6</sup> John T. Jayne,<sup>6</sup> Hugh Coe,<sup>1</sup> and Douglas R. Worsnop<sup>6</sup>

Received 22 March 2002; revised 2 July 2002; accepted 5 August 2002; published 4 February 2003.

[1] In part 1 of this series, techniques for generating quantitative information on fine airborne particulate-size and chemically resolved mass concentration from an Aerodyne aerosol mass spectrometer were introduced. Presented here are the results generated using these techniques from sampling U.K. urban air with such an instrument in Edinburgh during October 2000 and in Manchester during July 2001 and January 2002. Data on the total mass concentrations and size-resolved mass distributions of nitrate, sulfate, and organic compounds were obtained for all three campaigns and compared with data from other sources, including a micro-orifice uniform deposit impactor, total particle numbers, CO and NO<sub>x</sub> concentrations, local wind speed and temperature, and back trajectory analysis. All three locations showed evidence for emissions from local transport, with a mass modal aerodynamic diameter of around 100–200 nm. This mode was dominated by hydrocarbons showing little evidence of oxidization. The three sites also exhibited a larger mode consisting of inorganic chemicals and oxidized organics, which appeared to be governed by sources external to the cities and showed evidence of internal mixing. The mass modal aerodynamic diameter varied between approximately 200–500 nm during the winter and 500–800 nm during the summer. The summer also showed an increased mass loading without an increase in total particle number. Evidence of material building up and ageing in the atmospheric surface layer during periods of low wind speeds was also

observed. **INDEX TERMS:** 0305 Atmospheric Composition and Structure: Aerosols and particles (0345, 4801); 0345 Atmospheric Composition and Structure: Pollution—urban and regional (0305); 0394 Atmospheric Composition and Structure: Instruments and techniques; **KEYWORDS:** aerosols, chemical composition, urban, organic, mass spectrometry

**Citation:** Allan, J. D., et al., Quantitative sampling using an Aerodyne aerosol mass spectrometer, 2, Measurements of fine particulate chemical composition in two U.K. cities, *J. Geophys. Res.*, 108(D3), 4091, doi:10.1029/2002JD002359, 2003.

### 1. Introduction

[2] Urban areas have always been seen as a major source of particulate pollution [Colville *et al.*, 2001; Finlayson-Pitts

and Pitts, 1997; Mayer, 1999], which is expected to continue to increase due to world population growth and increasing industrialization and energy use, especially in developing countries [Fenger, 1999]. The direct impact of urban particulate pollution on human health has been the subject of much research and periods of high mortality and morbidity have been linked to elevated levels of particulate pollution [e.g., Dockery *et al.*, 1993; Schwartz, 1994]. Research has shown that long-term exposure to be detrimental to people's health and life expectancy [Nevalainen and Pekkanen, 1998; Pope *et al.*, 2002] and that short-term exposure may trigger problems such as heart failure in susceptible individuals [Peters *et al.*, 2001] and constriction of the arteries, even in healthy adults [Brook *et al.*, 2002].

[3] The monitoring of particulate air pollution has traditionally focused on particles of less than 10  $\mu\text{m}$  in diameter (the PM<sub>10</sub> standard), as these are more likely to pass the throat when inhaled [Department for Environment Food and Rural Affairs, 2001; Künzli *et al.*, 2000; Larssen *et al.*,

<sup>1</sup>Department of Physics, University of Manchester Institute of Science and Technology, Manchester, UK.

<sup>2</sup>Department of Chemical Engineering, University of Manchester Institute of Science and Technology, Manchester, UK.

<sup>3</sup>Department of Environmental Science and Engineering, California Institute of Technology, Pasadena, California, USA.

<sup>4</sup>Now at Department of Chemistry and Cooperative Institute for Research in the Environmental Sciences, University of Colorado, Boulder, Colorado, USA.

<sup>5</sup>Centre for Ecology and Hydrology Edinburgh, Penicuik, Midlothian, UK.

<sup>6</sup>Aerodyne Research Incorporated, Billerica, Massachusetts, USA.

1999] but it has become apparent that the smaller (“fine”) fraction is more significant, as these particles will penetrate deeper into the lungs and potentially cause more physiological distress or damage [Harrison and Yin, 2000; Seaton *et al.*, 1995]. This has led to the use of the PM<sub>2.5</sub> standard in countries such as the United States, where the total mass of fine particulate matter (less than 2.5  $\mu\text{m}$  in diameter) is monitored [Environmental Protection Agency, 1997]. While many techniques exist for the measurement of the size, number and mass of fine particulate matter in real time, studying its chemical nature has proven more difficult [Chow, 1995; McMurry, 2000].

[4] Of particular interest in the urban environment are organic compounds. These represent an important but poorly understood aerosol component compared to inorganic compounds such as nitrate and sulfate [Jacobson *et al.*, 2000; Turpin *et al.*, 2000]. Many studies have focused on quantifying the elemental carbon (EC) and organic carbon (OC) content of impactor or filter samples and the comparison of these quantities [e.g., Turpin and Huntzicker, 1991, 1995]. Both of these forms of carbon have been linked to anthropogenic emissions. Elemental carbon is a key component of primary carbonaceous particles, i.e., soot within primary particle emissions from combustion. Organic carbon has been found to be present in these particles but is also observed in particles having originated from gas to particle conversion processes (secondary organic particles). The OC to EC ratio can be calculated for primary carbon activity (e.g., Turpin and Huntzicker [1995] found the ratio to be approximately 2.18), and organic carbon levels above this have been used to indicate the presence of secondary organic compounds. A major source for these particle-phase chemicals is the low vapor pressure products of the oxidation of gas phase volatile organic chemicals by species such as O<sub>3</sub>, OH, and NO<sub>3</sub>. These processes are enhanced in the plumes of cities when precursors and radical concentrations are higher and in the case of OH and O<sub>3</sub>, during periods of strong sunlight when photolysis rates are elevated. The low-volatility products quickly condense onto existing particles or nucleate to form new particles [Seinfeld and Pandis, 1998].

[5] A major limitation of impactor and filter technologies is that the detection limits of the laboratory analysis instrumentation necessitate the collection of a large enough mass of sample for analysis, so temporal resolution is limited to greater than several hours for ambient samples. Also, the sample may be affected by evaporation or condensation of semivolatile components during or after sample collection and chemical reactions may take place within the sample itself or between oxidants in the sample gas and the collected particles, affecting the results [Chow, 1995; Zhang and McMurry, 1987, 1992]. The size resolution of these instruments is generally poor because of the limitations of aerodynamic particle separation and the need to increase sampling times and analyze a larger number of samples with increasing size resolution.

[6] Tandem differential mobility analyzers (TDMAs) and other particle hygroscopic growth measurement techniques have been used to show that in the urban environment, aerosol are typically externally mixed, displaying two separate modes of “less” and “more” hygroscopic particles [McMurry and Stolzenburg, 1989; Swietlicki *et al.*, 1999].

The less hygroscopic particles are those that exhibit little or no growth when exposed to a high relative humidity (RH) (typically 80–90%) and are thought to be mainly composed of hydrophobic chemicals such as water insoluble organic compounds and soot [McMurry *et al.*, 1996]. More hygroscopic particles grow by a larger factor (e.g., 1.38–1.69 for 35–265 nm particles at 90% RH [Swietlicki *et al.*, 1999]) and have been shown to contain inorganic chemicals such as nitrate, sulfate, sodium and potassium and sometimes, organic carbon as well [McMurry *et al.*, 1996]. The hygroscopic behavior of these particles is an important quality, as this will determine how they interact with clouds [Bower *et al.*, 2000], which, in turn, affects uptake of gaseous species, surface deposition, climate forcing, and the hydrological cycle [Ramanathan *et al.*, 2001]. Recent measurements in Pasadena by Cocker *et al.* [2001] have shown this two mode model to be somewhat simplified, as a range of hygroscopic particle growth behaviors was observed.

[7] Much chemical characterization of particles has been performed during recent years using laser desorption and ionization (LDI) based single particle aerosol mass spectrometers [e.g., Murphy and Thomson, 1995; Prather *et al.*, 1994]. These instruments have yielded detailed information on the nature of chemical mixing and aerosol speciation in real time [e.g., Liu *et al.*, 1997; Murphy *et al.*, 1998; Silva and Prather, 1997]. Unfortunately, these instruments have, to date, been limited to providing qualitative information only. Also, particles with optical diameters of 200 nm and below and some chemicals are difficult to study [Allen *et al.*, 2000; Kane and Johnston, 2000; Silva and Prather, 2000].

[8] The companion paper Allan *et al.* [2003] discusses methods of obtaining quantitative results from an Aerodyne aerosol mass spectrometer (AMS), described by Jayne *et al.* [2000] and Jimenez *et al.* [2003], on particulate mass with respect to both size and chemical composition. Unlike LDI-based instruments the AMS uses thermal desorption, electron impact ionization (EI) and quadrupole mass spectrometry. This combination of techniques allows quantitative data to be obtained for all particles successfully collected, however mass spectra of individual particles are not obtained. The instrument is also capable of sizing particles aerodynamically.

[9] In this paper, results from three sampling periods in two U.K. cities using these techniques are presented and discussed and compared with results using other techniques during these field experiments. The first of the three deployments was in Edinburgh, Scotland during the third Sources And Sinks of Urban Aerosol field campaign (SASUA 3) in November 2000. The other two deployments discussed in this paper were in the center of Manchester, England. The first sampling period at this site was during June 2001 and the second was during January 2002.

## 2. Experiment

### 2.1. Edinburgh Deployment

[10] The instrument was deployed in the city of Edinburgh, U.K., from the 31 October until 10 November 2000. The AMS was housed in the Observatory House on Calton Hill (55°57'18"N, 3°11'01"W), close to the center of the city and about 30 m above street level, during the SASUA project. The aim of the project was to study the production,

processing, and fate of aerosol in the large-scale urban environment. A more detailed description of the site and the project is given by *Dorsey et al.* [2002]. The scientific findings arising from the AMS data and those of other instrumentation during the experiment are discussed in detail by *Williams et al.* [In preparation for *Atmospheric Environment*, 2002]. The inlet is composed of a gauze-covered, upturned funnel at the sample end of a 2 m long 6.35 mm internal diameter tube. The AMS ran almost continuously with short downtimes for calibrations on the 1, 3, 4, 7, and 9 November, and averaged data were recorded every 30 min. A micro-orifice uniform deposit impactor (MOUDI) was deployed at the same location during part of the sampling period.

## 2.2. Manchester Deployment

[11] Ambient air was sampled through a standard PM<sub>10</sub> inlet on the roof of the University of Manchester Institute of Science and Technology (UMIST) main building, approximately 30 m above street level and located near the city center of Manchester, United Kingdom (53°28'35"N, 2°14'03"W). This site has been used previously by *Williams et al.* [2000]. The inlet was approximately 2 m above roof level and was connected to the instrument via a 25.4 mm internal diameter stainless steel tube approximately 7 m long. The inlet flow rate was nominally 17 L min<sup>-1</sup>, which was subsampled and introduced into the AMS through a 2.8 mm internal diameter stainless steel tube. A TSI 3025a ultrafine condensation particle counter (uCPC) was run concurrently during both experiments and a suite of permanently deployed meteorological instrumentation was maintained on the same rooftop. This included a Gill Solent sonic anemometer, a Vaisala temperature and humidity probe, a Didcot tipping bucket rain gauge, and a Skye silicon photocell pyranometer. The AMS ran from 14–25 June 2001 and 17–28 January 2002. During the June sampling period, the averaging time was 30 min, but this was reduced to 15 min for the January period. There were brief downtimes on 17 and 21 June due to recalibrations. A software failure on 26 January caused an interruption in data collection. The problem was detected and logging resumed the following day.

## 2.3. Aerodyne Aerosol Mass Spectrometer

[12] The AMS design is described in detail by *Jayne et al.* [2000] and *Jimenez et al.* [2003], and the instrument used in this work is presented in detail in the accompanying paper [*Allan et al.*, 2003], along with the tools for analyzing the results from the instrument and quantifying the errors. Some significant modifications to the AMS took place between the different experiments and these are outlined below. The instrument is capable of operating in two modes, mass spectrum (MS) mode and time of flight (TOF) mode. During MS mode, the mass spectrometer is scanned and the chopper wheel is removed from the particle beam. This allows a mass spectrum of the total aerosol ensemble to be obtained and chemical loadings for certain species calculated. During TOF mode, the mass spectrometer remains at a fixed  $m/z$  setting for a fraction of a second (several tens of cycles of the chopper wheel) while the beam is chopped. This allows size-resolved mass distributions for chemical species to be generated.

[13] After the Edinburgh campaign, the turbomolecular pump associated with the detection region was upgraded (from a Varian model Turbo-V70LP to V250) to reduce the background pressure and therefore improve the signal quality by reducing the noise due to the ionization of the background gases. Between the June 2001 and January 2002 deployments, several significant improvements were made to the AMS. The vacuum system was again improved to reduce the background pressure further, this time by the addition of two more turbopumps (a Varian Turbo-V70LP and an Alcatel ATH 30 hybrid) and the narrowing of the internal apertures. The quadrupole mass spectrometer was upgraded to a Balzers QMA 410 from the QMA 400 used in the other studies. This change offered improvements in the transmission of ions, especially in the high  $m/z$  regime. The aerodynamic lens design was also improved, offering better focusing of sub-100 nm particles. The change in lens design did not adversely affect the transmission of the larger particles, as the high diameter cutoff in both designs is dictated by the pinhole used to control the flow (X. F. Zhang, Aerodyne Research, Inc., personal communication 2002). The chopper slits were narrowed (from 3.5% of the circumference to 2%), to improve sizing resolution (J. L. Jimenez et al., Size resolution of the aerosol mass spectrometer, manuscript in preparation, 2003) (hereinafter referred to as Jimenez et al., manuscript in preparation, 2003). Finally, the flat molybdenum heater coated with multiple layers of molybdenum mesh was replaced with a porous tungsten heater in an inverted cone shape, to improve particle collection efficiency.

## 3. Comparison of Organic $m/z$ Channels

[14] The first paper in this series [*Allan et al.*, 2003] describes how the AMS can be used to calculate the mass distributions of nitrate and sulfate components as a function of particle size. The total sampled organic mass distribution cannot be derived so easily, as different organic species with different EI fragmentation patterns may contribute to the total organic mass in different amounts in different size ranges. As a result, the separate  $m/z$  channels that are sampled may exhibit different mass distributions in diameter space. It is therefore necessary to inspect the individual organic  $m/z$  channels sampled in time of flight mode before generating overall organic mass distributions.

[15] The AMS in MS mode has been shown to generate 70 eV EI mass spectra for organic chemicals very similar to corresponding spectra in databases such as that of the National Institute of Standards and Technology (NIST) (M. R. Alfara, UMIST, unpublished laboratory data, 2002; P. J. Silva, Aerodyne Research, Inc., unpublished laboratory data, 2002). In common with traditional EI analysis, nonaromatic hydrocarbons generate large signals in  $m/z$  channels such as 43, 55, 57, 69, and 71 in the AMS. Compounds with carbonyl functional groups containing such as ketones and aldehydes generate significantly larger signals in  $m/z = 43$  ( $\text{CH}_3\text{CO}^+$  or  $\text{CH}_2\text{CHO}^+$ ), relative to other channels. Carboxylic acids produce a signal in  $m/z = 45$  ( $\text{COOH}^+$ ), which is not observed with hydrocarbons. It has also been found that with the AMS, dicarboxylic acids produce a large signal at  $m/z = 44$  ( $\text{CO}_2^+$ ) (M. R. Alfara, UMIST, unpublished laboratory data, 2002; P. J. Silva,



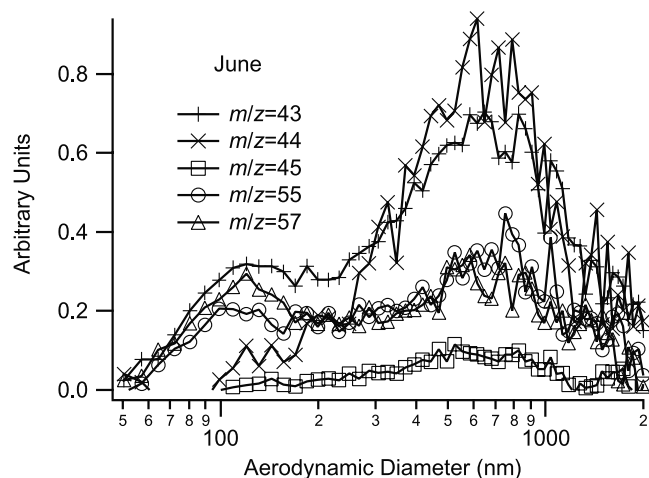


**Figure 1.** Comparison of the organic  $m/z$  channels in diameter space, averaged over the entire Manchester June 2001 campaign. The general distribution is bimodal, with the two peak heights varying depending upon the  $m/z$  channel. The lower peak is absent for  $m/z = 44$  and  $45$ .

Aerodyne Research, Inc., unpublished laboratory data, 2002), which does not appear when using conventional EI mass spectrometry [McLafferty and Turecek, 1993]. This fragment is produced for the entire class of compounds, and it is thought that this is an effect of the heated surface on the chemicals. This pattern is repeatable over a range of particle sizes and is suitable for quantitative analysis.

[16] The  $m/z$  channels chosen to study organic chemicals in TOF mode typically include  $m/z$  such as 41, 43, 44, 45, 55, 57, 69, and 71, based on the fact that these are prominent organic peaks in ambient mass spectra and are expected to arise from chemicals such as alkanes, carboxylic acids and alcohols [McLafferty and Turecek, 1993], which have been observed in ambient particles using other methods [Saxena and Hildemann, 1996]. When the channels were averaged over the entire June sampling period, two distinct mass modes were observed in diameter space, as shown in Figure 1. A summation of two lognormal

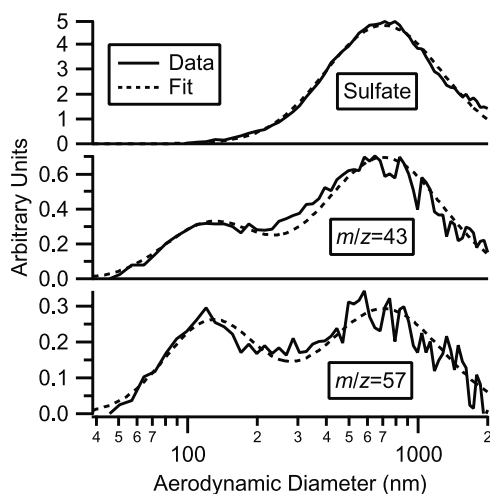


**Figure 2.** Examples of the lognormal curve fits to the signal distributions for the Manchester June 2001 campaign.

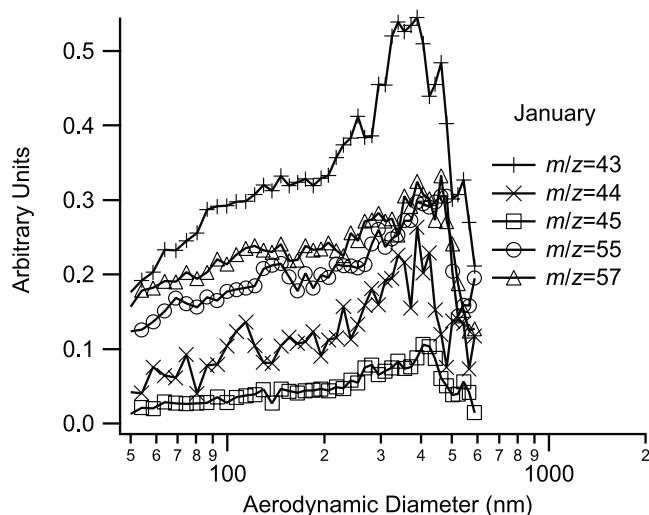


**Figure 3.** Comparison of the organic  $m/z$  channels in diameter space, averaged over the entire Manchester January 2002 campaign. The two peaks are again present, but they are less distinct compared to the June data, because of the reduced diameter of the higher mode.

distributions was used to model these observed distributions and used to calculate areas under the individual modes, which are representative of the mass loadings. Figure 2 shows some examples of the fits. The relative areas of the two modes vary between  $m/z$  channels. This ranges from the two modes being roughly equal in area for  $m/z = 57$  and  $55$ , the higher diameter mode being significantly larger for  $m/z = 43$ , to the smaller being virtually nonexistent for  $m/z = 45$  and  $44$ . When the analysis is repeated for the winter data, two modes also exist with a similar pattern in the relative signal sizes of the  $m/z$  channels (Figure 3). However, owing to the lower diameter of the larger mode, the two modes are less distinct. This analysis was not performed for the Edinburgh data because of the lower signal to noise of the data taken before the vacuum system upgrade and other instrument improvements. A summary of the relative sizes of the fitted peaks is shown in Table 1. These ratios are that of the lower diameter modes compared to the higher diameter modes. The lower ratios during the summer are indicative of the fact that the second, larger mode bears more mass during this sampling period, as will be discussed later. It appears that oxidized organics and inorganic chemicals are dominant in the larger mode, while nonoxidized organics have a larger presence in the smaller mode. When comparing the oxidized organic ratios with the nonoxidized, it appears that the effect is more pronounced during the summer. This implies that the oxidized organics have a greater presence during this season.

[17] The observation of bimodal size distributions suggests that at any one time, the total observable organic mass distribution as a function of  $\log(D_a)$ ,  $I(\text{org})$ , can be approximated as the sum of two lognormal modes. This can be summarized using the following equation:

$$I(\text{org})_{\log(D_a)} \approx a_{\text{org}} f_{\log(D_a)}^1 + b_{\text{org}} f_{\log(D_a)}^2, \quad (1)$$

where  $f^1$  and  $f^2$  are two modes in log diameter space of unit area and  $a_{\text{org}}$  and  $b_{\text{org}}$  are the sizes of the modes. It is also

**Table 1.** Ratios of the Equivalent Masses of the Fitted Lognormal Peaks for the Two Manchester Sampling Periods<sup>a</sup>

<i>m/z</i>	Source	Peak Ratios	
		January	June
30	nitrate	0.34	0.08
46	nitrate	0.42	0.08
48	sulfate	0.19	0.01
64	sulfate	0.16	0.01
98	sulfate and organics	0.81	–
15	ammonium	0.49	0.09
36	chloride	0.34	0.10
41	organics and oxidized organics	2.46	0.80
43	organics and oxidized organics	2.23	0.52
44	oxidized organics	1.30	0.12
45	oxidized organics	1.16	0.12
55	organics	3.59	0.92
57	organics	5.31	1.39
69	organics	3.89	1.21
71	organics	8.00	1.49
83	organics	4.95	1.23
85	organics	–	1.29

<sup>a</sup>The relative height of the first (lower diameter) peak is largest for organic species, followed by oxidized organics then inorganics. This is more distinct during June when the higher diameter mode bore more mass. The missing values are due to the *m/z* not being scanned.

assumed that the signal (ion rate) distributions from individual *m/z* channels also obey the same approximation using the same mode functions  $f^1$  and  $f^2$ . Ideally, a representative total organic mass distribution could be derived by scanning and summing up the distributions of all organic *m/z* channels in TOF mode. Since this approach is not practical for general use, however, the total organic distribution must be approximated by using the weighted summation of two or more distributions from organic *m/z* channels, using the method described below, before normalizing to the total organic loading.

[18] The *m/z* channels chosen for the determination of the total organic distribution must have high signal to noise and when combined with the appropriate weighting factors, must correctly represent the behavior of the total organic loading. The first requirement of high signal to noise is best fulfilled by *m/z* = 43, 55, and 57. The *m/z* = 44 and 45 channels have too low a signal to noise to be suitable for this analysis. The ability of the three channels to represent the total organic loading is checked by doing a linear least squares fit to equation (2):

$$I(\text{org})_{\text{total}} \approx p_{43}I(43)_{\text{total}} + p_{55}I(55)_{\text{total}} + p_{57}I(57)_{\text{total}}, \quad (2)$$

where  $I(\text{org})_{\text{total}}$  is the total organic mass loading, which is derived as a function of time from MS mode using the methods described in the companion paper [Allan et al., 2003],  $I(m/z)_{\text{total}}$  are the total signals from the respective *m/z* channels obtained as a time series from MS mode, and  $p_{m/z}$  are the weighting factors for each *m/z* channel determined from the fit. The fit produced using this method on the Manchester January 2002 data is shown in Figure 4. The fit is very good and the weighting factors  $p_{43}$  and  $p_{57}$  relative to  $p_{55}$  are found to be 1.46 and 0.57, respectively.

[19] The weighting factors are indicative of how much of the behavior of the total organics is represented by the activity in a particular *m/z* channel. Note that it is the relative sizes and not the total magnitude of these factors

that is important, as the final TOF distribution will be normalized to the total organic loading after summation. The area under the total organic distribution will be a sum of the areas of the two modes, as follows:

$$I(\text{org})_{\text{total}} \approx a_{\text{org}} + b_{\text{org}} \quad (3)$$

[20] If it can be assumed that the weighting factors,  $p_{m/z}$ , are constant within a measurement period, then the total organic mass distribution can be derived as a function of time using the following equation:

$$I(\text{org})_{\log(D_a)} \approx p_{43}I(43)_{\log(D_a)} + p_{55}I(55)_{\log(D_a)} + p_{57}I(57)_{\log(D_a)}, \quad (4)$$

where  $I(m/z)_{\log(D_a)}$  is the signal distribution of channel *m/z*. If the peak sizes within the individual distributions ( $a_{m/z}$  and  $b_{m/z}$ ) are separated, the following generalizations for  $a_{\text{org}}$  and  $b_{\text{org}}$  can be made, based on equation (1):

$$\begin{aligned} a_{\text{org}} &= p_{43}a_{43} + p_{55}a_{55} + p_{57}a_{57} \\ b_{\text{org}} &= p_{43}b_{43} + p_{55}b_{55} + p_{57}b_{57} \end{aligned} \quad (5)$$

Note that changes to the modal diameter or indeed the shape of the modeled distributions ( $f^1$  and  $f^2$ ) over time will not affect this approach, providing that any change is reflected equally in all *m/z* channels.

[21] The assumption that the weighting factors do not change within a sampling period seems to hold reasonably well, based on the quality of the fit in Figure 4. However, this is based on the assumption that any changes in the chemical makeup of the organic fraction can be accounted for in three degrees of freedom as three *m/z* channels are used to model the total. While this assumption will not strictly be true, this approach should be more than adequate as a first order approximation providing that the model described by equation (1) holds and the chemistry within each mode does not vary significantly with time. These leave the sizes of the two modes as the only independent

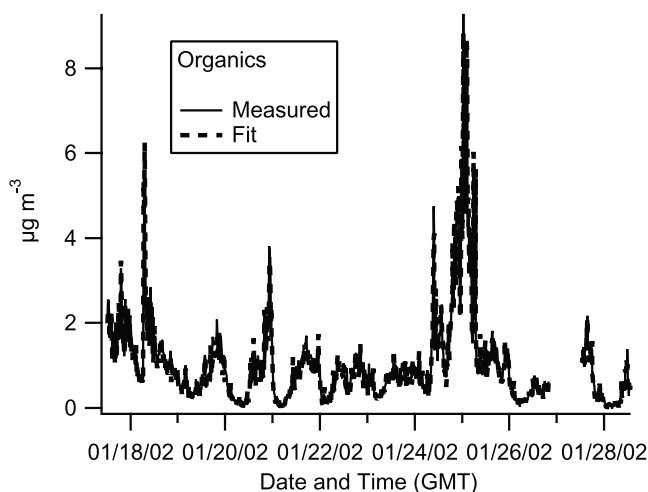


**Figure 4.** Comparison of the total organic mass loading to the approximation derived from the weighted summation of *m/z* channels 43, 55, and 57 (Manchester in January 2002).

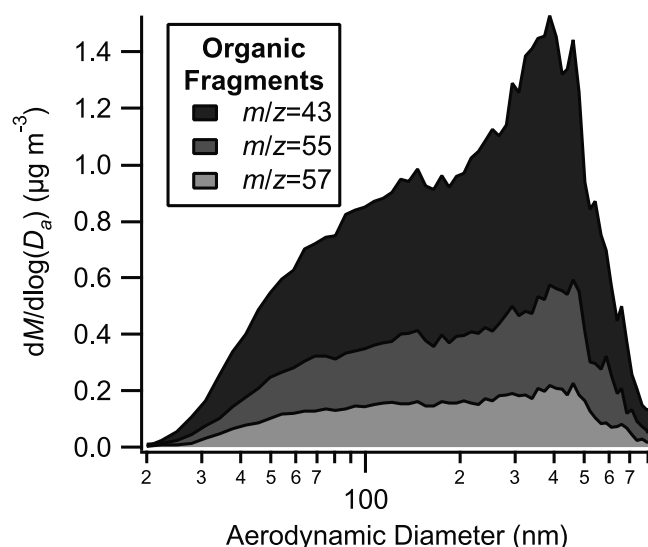


**Figure 5.** Example of how the  $m/z$  channels 43, 55, and 57 can be weighted and combined to form a representative organic mass distribution (Manchester in January 2002).

variables and therefore at least two degrees of freedom are necessary. An example of the final weighted summation of the signal distributions, after normalizing to the total organic loading, is given in Figure 5. Also shown are the fractional contributions from the different  $m/z$  channels.

#### 4. Detection Limits

[22] An estimate of the detection limits of the data can be made by performing the evaluation of the uncertainties in MS signals as described by *Allan et al.* [2003] on the raw MS data and from that, calculating the errors associated with the nitrate, sulfate, and organic mass concentration, calculated from each campaign. There will be a minimum uncertainty value for each data series because when the mass concentration is zero (or near zero), background gas phase material will still be present in the instrument and causing apparent noise. The January 2002 data set had several suitable periods such as these and the  $3\sigma$  detection limits for this campaign can be taken to be three times the error values during these periods. These were calculated for nitrate, sulfate, and organics to be  $0.006$ ,  $0.015$  and  $0.041 \mu\text{g m}^{-3}$ , respectively. Note that this applies to 15 min sampling periods; an increase in the sampling time will result in a reduction in the detection limit.

#### 5. Edinburgh Results

[23] The time series of the total loadings derived from MS mode in Edinburgh using the methods described by *Allan et al.* [2003] are shown in Figure 6 and can be divided into three main periods. In the period from the start of the experiment to 6 November, the local wind advected air mainly from the center of the city to the site. The measured aerosol mass was dominated by organic compounds, with an average concentration of  $0.89 \mu\text{g m}^{-3}$ , but some sulfate and nitrate were also present with average concentrations of  $0.46 \mu\text{g m}^{-3}$  and  $0.18 \mu\text{g m}^{-3}$ , respectively. On the 6 November, the conditions changed and the air was

principally advected off the North Sea. During this period, the nitrate loading dropped to about  $0.03 \mu\text{g m}^{-3}$ , while the sulfate and organics remained significant at around  $0.7 \mu\text{g m}^{-3}$  and  $0.3 \mu\text{g m}^{-3}$ , respectively. On 9 November the wind direction was again over land, and the nitrate loadings increased.

[24] Of particular note is the night of 5 November (known in the United Kingdom as “Bonfire Night”), when the measurement site was directly downwind of a very large firework display at the Meadowbank stadium in Edinburgh, which resulted in a number of unusual signals in the mass spectrum, as shown in Figure 7. An initial examination shows very high signals due to potassium, sulfate, and organics, which compares well with similar measurements and analysis of pyrotechnically derived aerosol performed by *Liu et al.* [1997] using an aerosol time of flight mass spectrometer (ATOFMS). Note that potassium has an unrealistically large signal, approaching that of oxygen. This is because  $\text{K}^+$  ions were being formed in large numbers on the surface of the heater rather than by the electrons from the filament. This “surface ionization” is undesirable, as it does not produce quantitative data. It has been found that this effect can be overcome by adjusting the temperature and voltage bias of the heater.

[25] The  $dM/d\log(D_a)$  distributions as a function of time derived from the analysis of the time of flight mode data are shown as a color image plot in Figure 8. The time series of the sulfate distribution shows that for the first period of urban air, the mass mode is at an aerodynamic diameter of about 400–500 nm. During the marine period, the mode center drops to 300–400 nm, while during the final urban period it reduces further to 200–300 nm. The nitrate distribution is much broader and has a varying peak location, but the mode generally spans between 100 and 600 nm. The organics displayed two modes, the smaller diameter mode occurring typically between 100 and 200 nm, stretching down to about

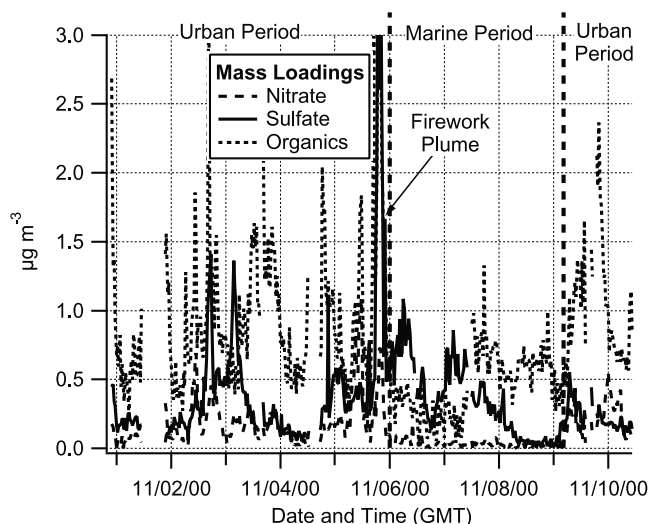


**Figure 6.** Calculated mass loadings of nitrate, sulphate, and organics from Edinburgh during November 2000. The large amount of activity on 5 November due to a firework plume is indicated. During the indicated period from 6–9 November, the air was mainly advected off the North Sea. At other times, the air came off the city.



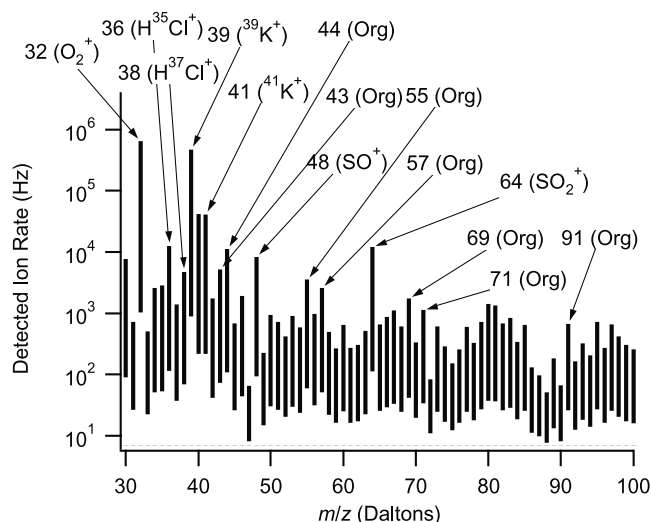


**Figure 7.** Mass spectrum up to  $m/z = 100$  taken during bonfire night (5 November), Edinburgh, 2000. The large signals are labeled, most notably potassium (K). Fragments due organic chemicals are labeled “Org.” The lower ends of the sticks correspond to the calculated  $1\sigma$  error values, as described by Allan *et al.* [2003].

70 nm. The lower end of the distribution is probably more indicative of the size cutoff of the aerodynamic lens used in this study rather than the ambient distribution itself, due to the low focusing efficiency of particles of this size (see the first graph in Figure 10). The second mode occurred at the same aerodynamic diameter as sulfate. The organic distributions tended to be very broad, often reaching  $1\mu\text{m}$ . However, information on organic distributions from this campaign is

limited because few  $m/z$  channels were being scanned in TOF mode. Also, the heater was operated at a temperature of approximately  $950^\circ\text{C}$ , resulting in excessive decomposition of organic molecules on the surface of the heater, causing information on the nature of the parent chemicals to be lost. During the Manchester June and January experiments, temperatures of  $650^\circ\text{C}$  and  $400^\circ\text{C}$ , respectively, were used.

[26] The MOUDI operated over six sampling periods at the Edinburgh site during the AMS sampling period. The ion chromatography (IC) derived mass concentration data for nitrate and sulfate for the MOUDI substrates were taken and compared to the AMS data in Figure 9. The bold lines show the AMS-derived mass loadings averaged over the MOUDI sampling periods. The mass loadings from the bottom three stages of the MOUDI were summed, giving a total chemical loading of particles of an aerodynamic diameter less than 526 nm. This was chosen because it most closely represents the particles the AMS is capable of observing, but total agreement is not expected, as the AMS observes some particle mass between 526 and 1000 nm, albeit with a reduced efficiency. Note that a factor of 2.5 is applied to the sulfate measurements, as described by Allan *et al.* [2003]. The Pearson’s  $r$  values (equation (14.5.1) of Press [1992], also known as linear covariance) were calculated for these series, to quantify the agreement (a scale where 1 is perfect correlation, 0 is no relationship and  $-1$  is perfect anticorrelation). The quantitative agreement between the instruments for nitrate is fair ( $r = 0.67$ ) but is better for sulfate ( $r = 0.82$ ), the major exception being the period encompassing 5 November. This discrepancy will almost certainly be due to an effect caused by the abundance of firework-derived particles, although the precise mechanism for this can only be guessed at.

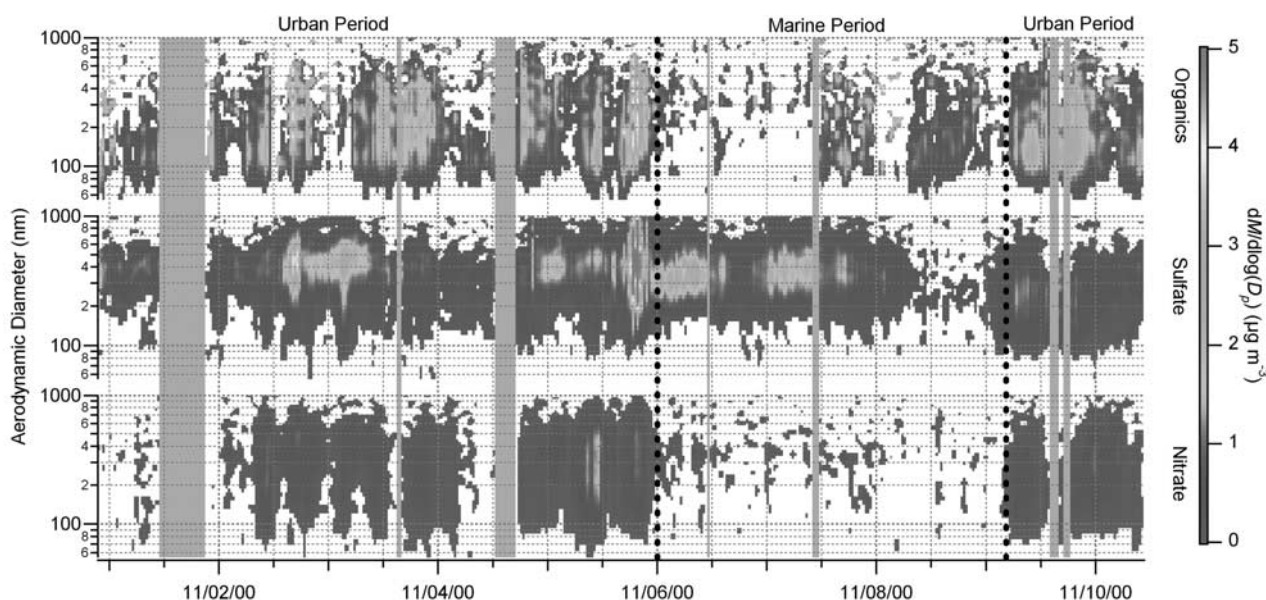


**Figure 8.** Calculated mass distributions of nitrate, sulfate, and organics from Edinburgh during November 2000. The data have been smoothed using a  $2 \times 2$  point Gaussian method, and data points below a calculated  $2\sigma$  threshold level (as described by Allan *et al.* [2003]) have been removed to improve clarity. See color version of this figure at back of this issue.

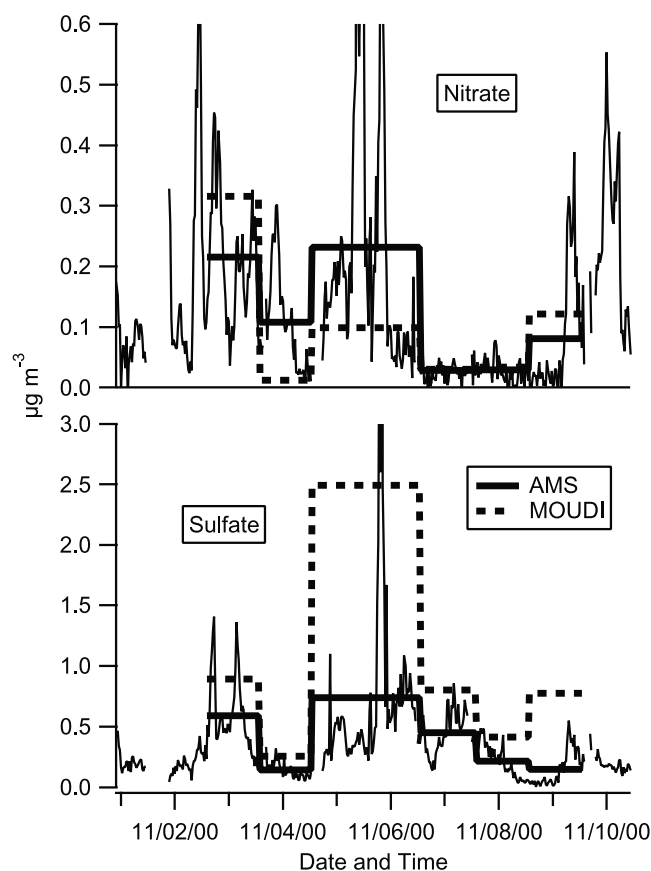


**Figure 9.** Comparison of total loadings from SASUA 3 with the equivalent micro-orifice uniform deposit impactor (MOUDI) data, summed over the bottom three stages ( $<526$  nm). The bold solid lines represent the aerosol mass spectrometer (AMS) measured loading averaged over the MOUDI sampling periods. There is some disagreement in the nitrate loadings, but the agreement in the sulfate is good, except for the period encompassing the firework plume.

[27] It is unclear whether the discrepancies in the measured nitrate arise from either the MOUDI or the AMS. It is, however, possible that evaporation or condensation of ammonium nitrate, a semivolatile species, on the MOUDI substrates could be taking place, as this is an effect that is commonly observed with impactors [Zhang and McMurry, 1987, 1992]. The AMS shows that the ambient concentration varied considerably within the MOUDI sampling periods. It is worth noting that the sampling periods in Figure 9 in which it was observed that the MOUDI sample contained less nitrate than the AMS measurement all ended at times of low nitrate concentration (the sample change-overs on 3 and 9 November). Conversely, when the MOUDI samples were observed to contain more nitrate than the AMS measurement, the sampling periods ended at times of elevated concentration (4 and 6 November).

[28] The mass from the samples has been converted to  $dM/d\log(D_a)$  distributions and the AMS mass distribution traces have been averaged over the MOUDI sampling periods to provide a direct comparison of results for nitrate and sulfate mass distributions in diameter space. Some examples are shown in Figure 10. The lens transmission

function, i.e., the predicted particle focusing efficiency as a function of aerodynamic diameter as described by Jayne *et al.* [2000], is also shown on the graph to indicate the regimes in which the AMS operates at reduced efficiency (X. F. Zhang, Aerodyne Research, Inc., personal communication 2002). Note that this function applies to the instrument configuration used in Edinburgh and that the lens design used during the Manchester January campaign offers an improvement in the small particle regime.

[29] The AMS observes little of the material of sizes greater than  $1\text{ }\mu\text{m}$ , which is expected. With sulfate, there is good agreement between the two instruments in the accumulation mode ( $D_a < 1\text{ }\mu\text{m}$ ), with the peaks being of similar heights and only small disagreement between the modal diameters. The AMS measured reduced loading in the upper tail of the mode ( $>500$  nm) but this corresponds to the reduction in the lens transmission efficiency at these sizes. The data were not corrected for this, as this regime will be affected by both chopper broadening and the finite vaporization time of

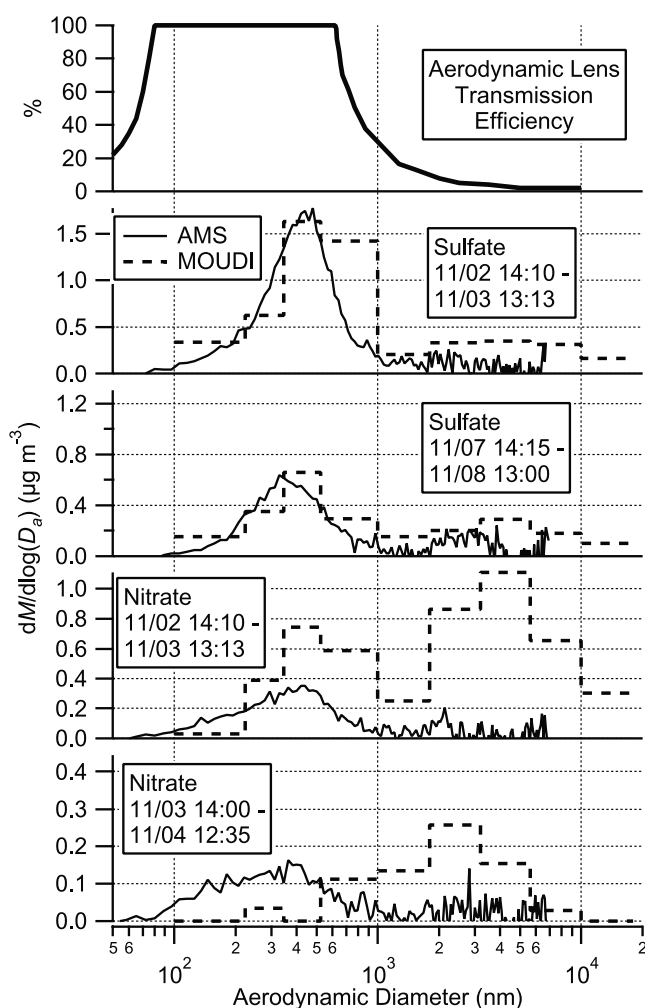


**Figure 10.** Examples of MOUDI mass distributions compared with AMS mass distributions, averaged over the same sampling periods. The lens transmission curve described by Jayne *et al.* [2000] is also shown, predicting the regime in which the AMS will detect particles with 100% efficiency. Again, the sulfate agreement is good, whereas the nitrate displays some discrepancies.



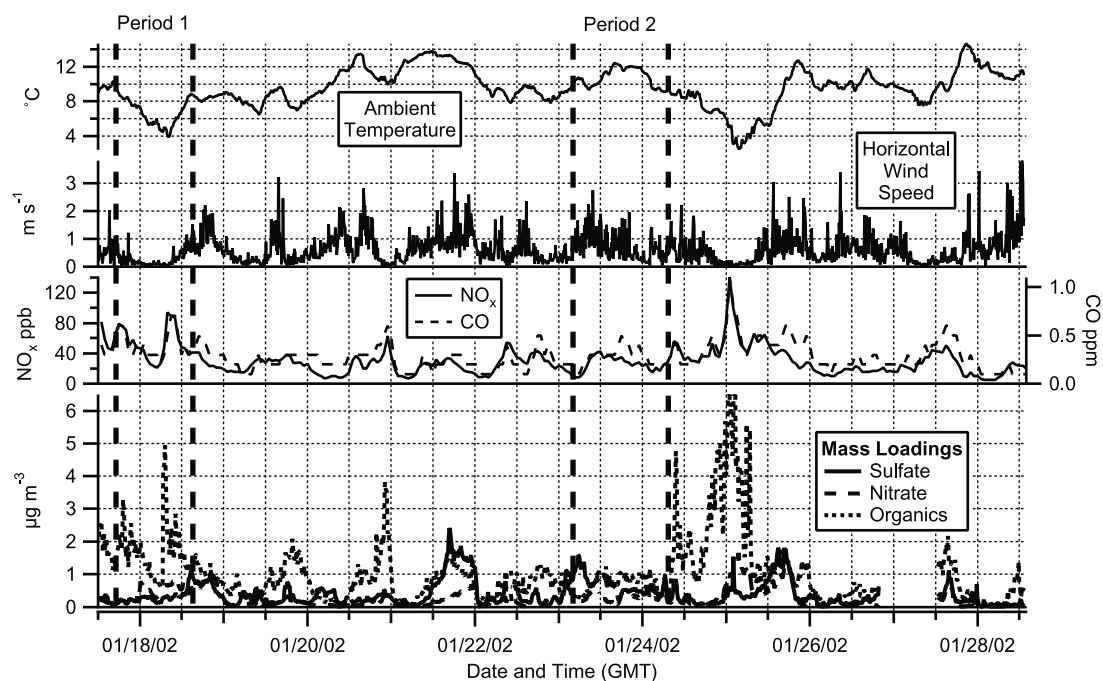


**Figure 11.** AMS mass loadings from Manchester for January 2002 and auxiliary data. Periods 1 and 2 are sample periods of low and high wind speed, respectively.

larger particles, which has the effect of broadening the high diameter end of the distributions (Jimenez et al., manuscript in preparation, 2003). It is not possible to correct for size-dependent lens transmission without first taking these phenomena into account and the techniques for doing this are currently still under development.

[30] There are some disagreements with the nitrate, as discussed above. While positive and negative artifacts on the MOUDI due to exchanges with the gas phase are a possibility, there may be other issues at play regarding either

instrument that have yet to be identified and accounted for, such as inlet issues and particle bounce.

## 6. Winter Manchester Results

[31] The time series of total mass and mass distributions as a function of particle aerodynamic diameter are presented in Figures 11 and 12, respectively, together with collocated measurements of ambient temperature and horizontal wind speed (from the meteorological instruments on the roof of

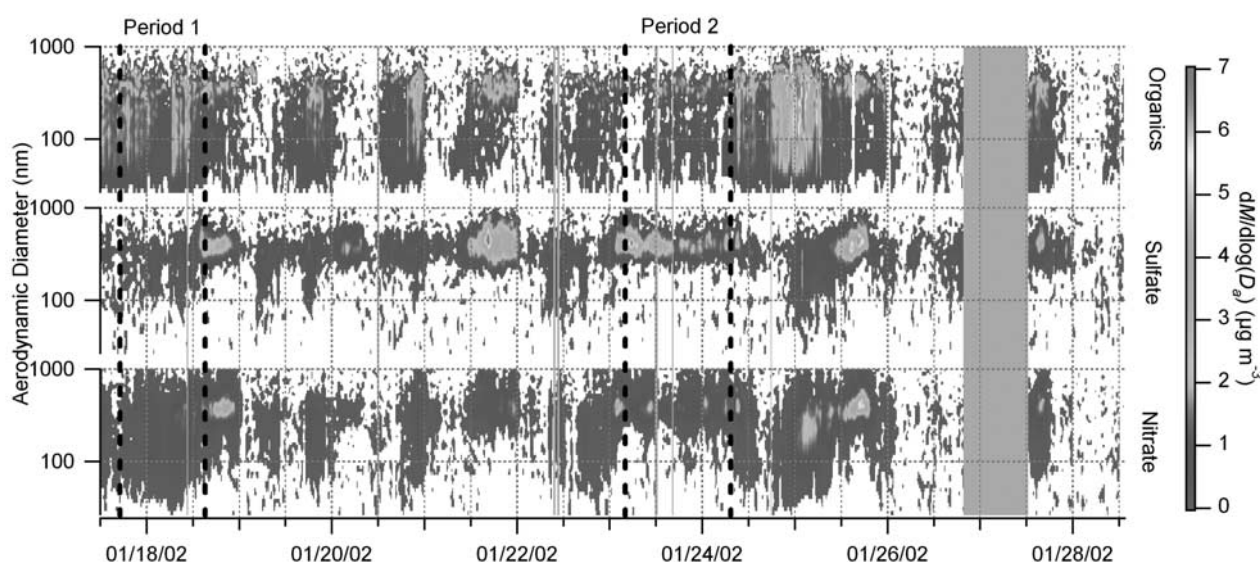


**Figure 12.** Calculated mass distributions from Manchester for January 2002. A smoothing and filtering process identical to that used for the Edinburgh data has been applied. See color version of this figure at back of this issue.

the UMIST main building) and  $\text{NO}_x$  and CO concentrations. The gas measurements were provided by an automated Department of the Environment, Transport and the Regions monitoring site on the roof of Manchester Town Hall, located approximately 0.75 km away in the city center ( $53^\circ 28' 43'' \text{N}$ ,  $2^\circ 14' 40'' \text{W}$ ) 25 m above street level.

[32] These results display some similarities with the Edinburgh data set. The species loadings were slightly higher, though rarely above  $2 \mu\text{g m}^{-3}$ , except during some particular organic events, corresponding with periods of low wind speeds and high CO and  $\text{NO}_x$ . There is a persistent mode at around 400–500 nm, which is observed in nitrate, sulfate, and organics.

[33] Frequently, an additional organic mode of diameter 100–200 nm was present. This mode extended down to about 30 nm, which is the lower limit of the aerodynamic lens used during this sampling period. This mode is very strongly correlated with CO and  $\text{NO}_x$ , which themselves are well correlated within this campaign ( $r = 0.79$ ) and for all wind directions (D. W. F. Inglis, UMIST, personal communication 2002). These are good tracers for transport-related emissions. The U.K. Air Quality Statistics Database and National Atmospheric Emissions Inventory (NAEI) list that during 1999, transport was the producer of 69% and 44% of CO and  $\text{NO}_x$ , respectively, on a national level and 92% and 73% of the emissions within Manchester. The integrated organics of aerodynamic diameter less than 200 nm were compared with the CO and  $\text{NO}_x$  concentrations. These comparisons had Pearson's  $r$  values of 0.65 and 0.77, respectively. By performing a linear least squares fit to the  $\text{NO}_x$  (Figure 13), the slope was found to be  $0.0211 \mu\text{g m}^{-3} \text{ ppb}^{-1}$ , and the intercept was found to be  $0.128 \mu\text{g m}^{-3}$ . If it can be assumed that the majority of  $\text{NO}_x$  is primarily emitted by traffic in the form of NO, a mass emission ratio of 0.0172 for particulate organic matter to  $\text{NO}_x$  is found for Manchester traffic. Applying this to data

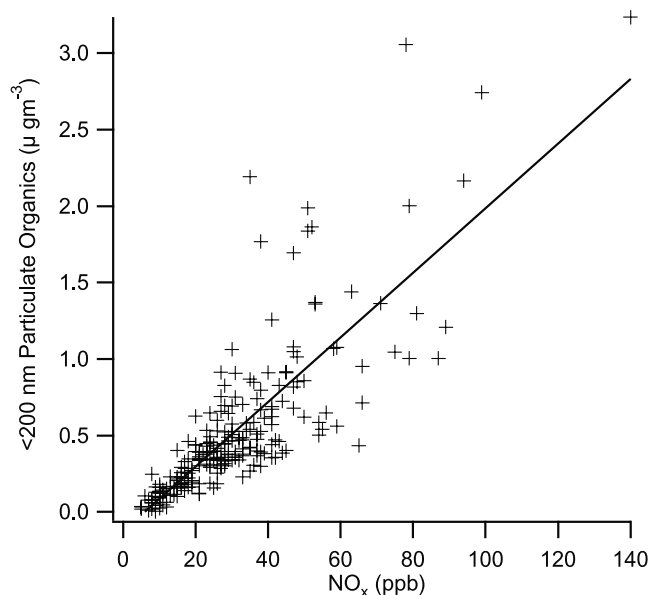


**Figure 13.** The integrated organic signal below 200 nm plotted against the  $\text{NO}_x$  concentration with the fitted line. The slope is  $0.0211 \mu\text{g m}^{-3} \text{ ppb}^{-1}$ , and intercept is  $0.128 \mu\text{g m}^{-3}$ .

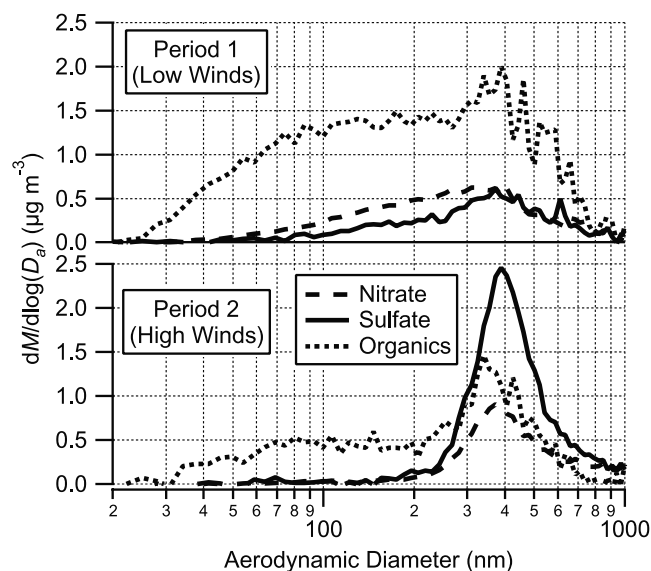


**Figure 14.** Comparison of the mass distributions of sulfate, nitrate, and organics during periods of differing meteorological conditions in Manchester for January 2002. The averaging periods are those marked on Figures 9 and 10.

from the NAEI, this corresponds to an estimated emission rate of  $0.45 \text{ t km}^{-2} \text{ yr}^{-1}$  of particulate organics from transport in Manchester. This is of a similar order as the NAEI quoted  $\text{PM}_{10}$  emission rate of  $1.38 \text{ t km}^{-2} \text{ yr}^{-1}$  from Manchester transport. A similar fit to CO data gives a slope of  $2.29 \mu\text{g m}^{-3} \text{ ppm}^{-1}$ , an intercept of  $-0.158 \mu\text{g m}^{-3}$ , and an emission ratio of 0.00174.

[34] During some periods, the nitrate and sulfate distributions also exhibited an additional, lower aerodynamic diameter mode, which is not observed with these species at other times. These events normally occurred during periods of reduced temperatures and low horizontal wind speed. A graph comparing one such period (marked as period 1 on Figures 11 and 12) with a period of significant and steady local wind (period 2) is shown on Figure 14. During period 1, little mixing occurred, and a stable layer formed over the city, retaining urban emissions of gases and particles that were not removed by advection and accumulated to significant concentrations. It is possible that the presence of these particles may be due to a different type of emission during these periods, but it is more likely that the existing lower-diameter mode aerosol particles are being processed in situ, and so the observed changes in species mass loadings and size distributions between the two situations may be explained to some extent by gas to particle conversion.

## 7. Summer Manchester Results

[35] The results from the June experiment in Manchester are shown on Figures 15 and 16. The nitrate and sulfate loadings are significantly higher than in the other data sets, frequently reaching  $6 \mu\text{g m}^{-3}$  or higher. During periods when the nitrate and sulfate loadings are above  $2 \mu\text{g m}^{-3}$ , the main peak in the accumulation mode typically occurs at an aerodynamic diameter of 700–800 nm. This is signifi-

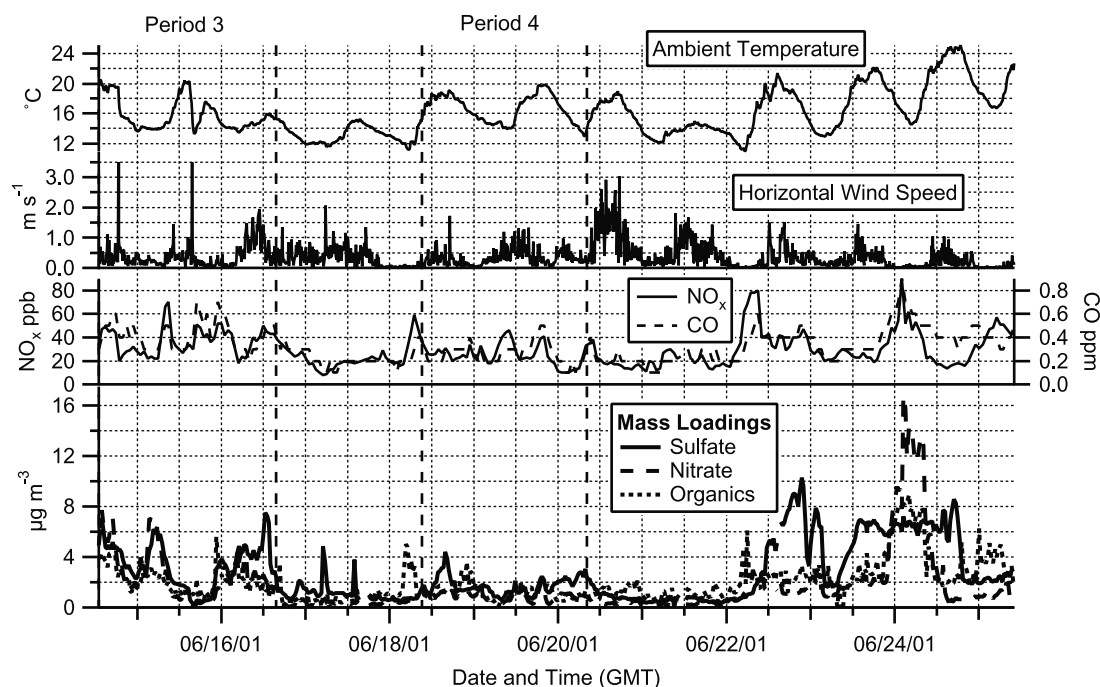


**Figure 15.** AMS mass loadings from Manchester for June 2001 and auxiliary data. Periods 3 and 4 are sample periods of high and low sulfate activity, respectively.

cantly larger than the particles observed in Edinburgh or Manchester during the winter. When the nitrate and sulfate loadings are below  $2 \mu\text{g m}^{-3}$ , their main mass mode occurs at approximately 500–600 nm. The average particle number concentration in the summer experiment as measured by the uCPC was almost identical to the January levels ( $1.63 \times 10^4 \text{ cm}^{-3}$ , compared to a winter average of  $1.62 \times 10^4 \text{ cm}^{-3}$ ),

confirming that the extra mass was due to the increase in size of the particles, rather than particle number.

[36] There were occasions when the sulfate levels were elevated for extended periods of time, most notably around 14–16 and 22–24 June. The former period is marked on the time series graphs as period 3, along with a contrasting low-activity period (period 4) from 18–20 June, and the mass

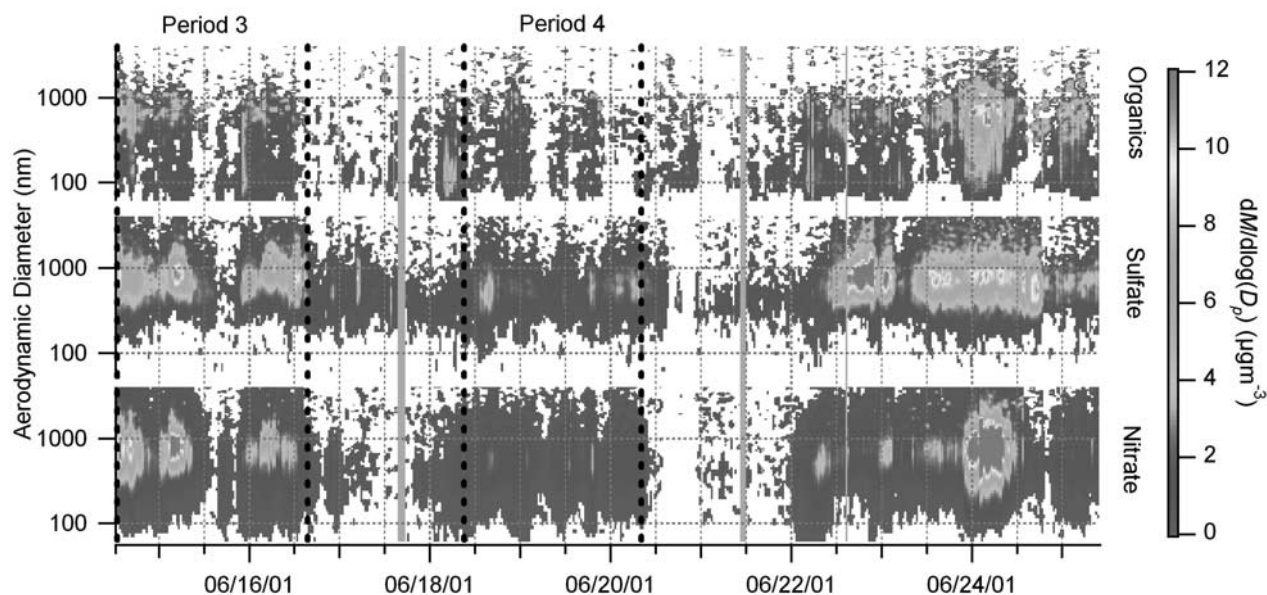


**Figure 16.** Calculated mass distributions from Manchester for June 2001. The same smoothing and filtering process has been applied as previously. See color version of this figure at back of this issue.



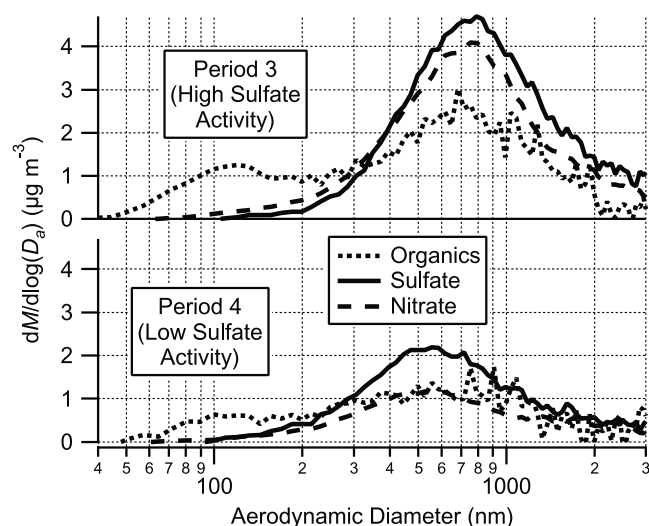


**Figure 17.** Comparison of the mass distributions of nitrate, sulfate, and organics from a high sulfate activity period (period 3) with those from a low sulfate activity period (period 4) from Manchester for June 2001.

distributions are compared in Figure 17. The sulfate mode increases in diameter from approximately 500 nm to 800 nm, and the corresponding modes in the organics and the nitrate do likewise. The chemical masses of the modes also increase significantly. The back trajectories in Figure 18 show that period 3 coincided with air that had traveled across other areas of Britain, picking up much pollution. The time taken for  $\text{SO}_2$  to convert to sulfate will be very short in the presence of nonprecipitating cloud [Chandler *et al.*, 1989], which was present over the region on these days (this was confirmed by the pyranometer and rain gauge data). The NAEI lists three  $\text{SO}_2$  point sources to the south of Manchester in the West Midlands that emit in excess of  $26,000 \text{ t yr}^{-1}$ , one of which emits more than  $50,000 \text{ t yr}^{-1}$ . There are 11 point sources that emit greater than  $50,000 \text{ t yr}^{-1}$  to the east. During times of low sulfate levels, the air typically came from over Wales and other areas to the west, where there are no significant point sources listed.

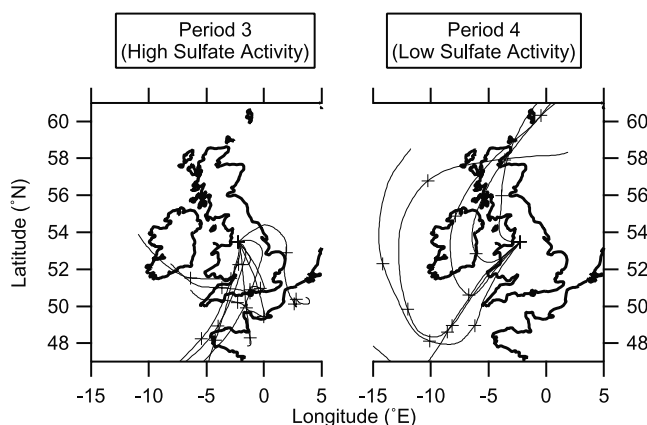


**Figure 18.** Four day back trajectories of the low sulfate activity and high sulfate activity periods from Manchester for June 2001. Markers are at 24 hour intervals.

[37] The organic fraction again exhibited a smaller mode at around 100–200 nm. However, as the main accumulation mode is shifted to a much higher diameter, it is now clearly a distinct mode. Like the January sampling period, the smaller mode is greatest during periods of low wind speed, meaning that it is most likely due to the build up of primary particle pollution from vehicle emissions.

[38] The largest particle event occurred from 2300 23 June until 1100 on 24 June. Figure 19 shows the mass distribution compared with that immediately prior. During this period, the temperature was low and the horizontal wind speed was negligible, implying that the air was stagnant in a relatively small surface layer over the city. This also occurred during a period when there was an abundance of 700 nm particles, mainly composed of sulfate. The total nitrate loading increased from  $2 \mu\text{g m}^{-3}$  to peak at  $14 \mu\text{g m}^{-3}$ , and the organics rose from  $3 \mu\text{g m}^{-3}$  to peak at  $8 \mu\text{g m}^{-3}$ . The sulfate loading remained stable at  $5 \mu\text{g m}^{-3}$ . During the increased nitrate and organic activity, the main mode increased in diameter slightly to 800 nm. The organics manifested a smaller mode at 100–200 nm, but the majority of extra nitrate and organic mass was present in the larger mode. The addition of this mass was either due to a local source of new particles or the condensation of gas phase material onto existing particles. The fact that the three chemical species share the same approximate modal diameter with similar mode shapes suggests the latter.

[39] The general assumption that the nitrate, sulfate, and organics are internally mixed in the higher mode for the entire campaign can be tested by looking at the mass modal diameter as a function of time. A lognormal fit was performed to 6 hour rolling averages of all three mass distributions, discounting all the mass below 300 nm (the high separation of the modes during this sampling period allowed this) and data series generated for the mode diameters as a function of time. Outliers of  $<400 \text{ nm}$  or  $>1500 \text{ nm}$  were discounted as bad data, as were points where the peak height was less than  $1 \mu\text{g m}^{-3}$ . However,

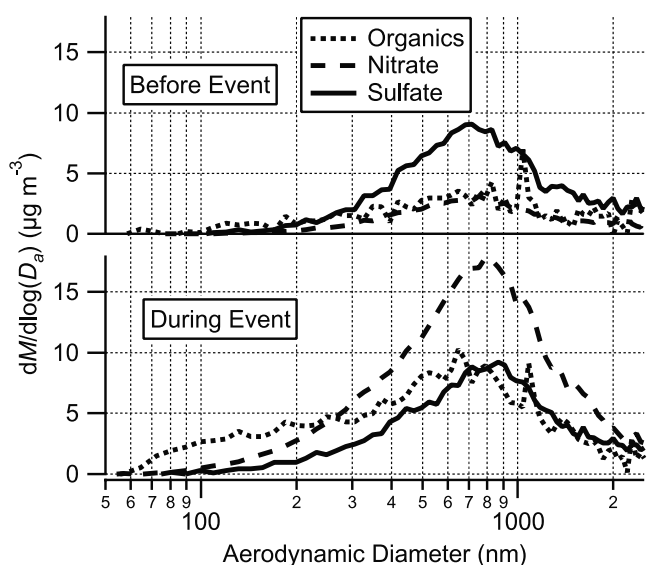


**Figure 19.** Nitrate, sulfate, and organic mass distributions from before and during the particle event on 24 June 2001 in Manchester.

even with these filters, the data series still contained a lot of random noise, especially that of the organics. The mean diameters of the nitrate, sulfate, and organic modes were  $697 \pm 96$  nm,  $657 \pm 125$  nm, and  $619 \pm 101$  nm, respectively, which are very similar. Despite the noise on the data series, positive covariance was found between the  $\log_{10}$  diameters of the nitrate and sulfate modes ( $r = 0.62$ ) and the organic and sulfate modes ( $r = 0.33$ ), showing that the mode diameters were not independent.

[40] While the results arising from this instrument alone cannot conclusively prove that the nitrate, sulfate, and organics are internally mixed, it does present strong evidence to support this hypothesis. A single particle instrument such as an aerosol time of flight mass spectrometer (ATOFMS) could shed light on this issue, and a data comparison between an instrument such as this and an AMS sampling at the same location would prove very interesting.

## 8. Discussion

[41] By comparing the three data sets, some distinct similarities and differences are evident. The size and nature of the 100–200 nm mode in all three campaigns appears to be consistent, being a mode consisting of hydrocarbons that can be linked to traffic emissions. This is consistent with results obtained by *Kleeman et al.* [2000], who studied motor vehicle emissions using an optical particle counter (OPC), a differential mobility analyzer (DMA), and a MOUDI, in which different engine types produced a mode at 100–200 nm, consisting mainly of OC. They found diesel engine emissions also contained a significant portion of EC, but the AMS was not expected to observe this component, as the heater will not have been hot enough to vaporize it. *Tobias et al.* [2001] also studied particles in diesel engine emissions with a thermal desorption particle beam mass spectrometer. They found that the particles of mobility diameter 25–60 nm were mainly composed of hydrocarbons, originating from unburned fuel and lubricating oil. This also agrees with *Williams et al.* [2000], who found that Manchester ambient particle number concentrations of the size range 100–500 nm to be linked to traffic activity. Particles freshly emitted from engines are generally hydrophobic [*Weingartner et al.*, 1997], so this corresponds to the “less hygroscopic” mode commonly observed in urban environments with TDMA.

[42] The observed particles of the larger diameter mass mode appear to consist of inorganic and partly oxidized organic chemicals. There is much variation in the size and nature of these particles, both within sampling periods and when comparing different periods. The fact that the modes of the different chemicals consistently occur at the same diameter suggests that they are internally mixed. This agrees with *Liu et al.* [2000], who observed organic material internally mixed with fine nitrate aerosol with an ATOFMS. During the summer in particular the size and mass loading of these particles increased dramatically compared to the winter, implying that there was a greater availability of the precursor chemicals. This will definitely be true of species such as secondary organic compounds, as many of these are produced through series of reactions that are dependent on sunlight. The presence of signals at  $m/z = 44$  and  $45$  in this

mode, which are indicative of oxidized organic species, supports the assumption that these chemicals are present in this mode. Also, the averaged ratio of the  $m/z = 43$ , and  $57$  signals from MS mode is larger during the summer (2.34, compared to 1.88), which qualitatively suggests that oxidized organic chemicals represented a larger fraction of the total organic mass concentration, although other differences in the nature of the organic chemicals such as chain lengths may also contribute to the changes in this ratio. The initial sources of the particles appear to be external to the cities, but sources within the cities may add to the mass of the mode.

[43] The separation of the two modes, especially in summer, is in part because of the aerodynamic sizing, which depends on both particle diameter and density. If the accumulation mode particles consist mainly of chemicals such as ammonium nitrate or sulfate, its density will be greater than if its main constituents were organic compounds. *McMurry et al.* [2002] also found by combining a TDMA with an aerosol particle mass analyzer (APM), “more hygroscopic” ambient particles tend to be of a higher density than the “less hygroscopic.” It is also known that the “less hygroscopic” particles tend to be very irregular in shape [*McMurry et al.*, 1996; *Weingartner et al.*, 1995] so will therefore be less aerodynamic compared to “more hygroscopic” particles, which tend to be spherical. These factors mean that an external mixture of organic and inorganic particles of similar geometric diameter will produce two distinct modes in aerodynamic diameter space. The fact that at any one time, the mass modes of nitrate, sulfate, and the larger organics occur consistently at the same aerodynamic diameters, when a change in composition would cause separation of the modes due to changes in density, implies that they are internally mixed. If the particles were externally mixed but had a high water content, they would conceivably have a similar density, but they are not expected to have the same modal diameter at a given humidity, as their hygroscopic properties are likely to be different. In addition, some of the water is likely to be lost in the low pressure of the lens before sizing occurs. Note that the typical relative contributions of the different chemicals to the higher mass mode do not vary greatly between summer and winter, so the seasonal change in the aerodynamic diameter of this mode is a not merely a reflection of the changes in the density of the particles.

[44] The in situ ageing of the particles in the lower mode observed is of particular interest. *Weingartner et al.* [1995] found that over a period of hours, the growth factor (when exposed to 90% relative humidity) of combustion-produced particles in a controlled environment gradually increased. It is known that after sufficient ageing, particles in polluted air no longer exhibit a “less hygroscopic” mode when analyzed with a TDMA [*Bower et al.*, 2000]. The implication is that the process observed is the initial stages of the particles being transformed into those like the older, higher diameter mode particles, containing significant inorganic and oxidized organic mass.

## 9. Conclusions

[45] Using mathematical techniques outlined in the accompanying paper *Allan et al.* [2003], data from the

cities of Edinburgh and Manchester in the United Kingdom during different seasons were analyzed and quantitative results presented. Detailed information on chemical loadings and size distributions for nitrate, sulfate, and organics were derived with high time resolution. A comparison of the Edinburgh results with the equivalent data from a colocated MOUDI was made.

[46] The observed nitrate, sulfate, and organic activity appeared to be confined to two modes during all campaigns. The lower diameter mode had a mass peak at an aerodynamic diameter of 100–200 nm and mainly consisted of organic chemicals with little oxidation. The organic activity in this mode correlated well with CO and NO<sub>x</sub> activity, meaning that it probably originates from motor vehicle emissions. Concentrations increased at times of low temperature and wind speed, implying pollutants were trapped in a surface layer and were not being dissipated by the wind. During these periods, processing of these particles was observed.

[47] The larger diameter mode occurred at various diameters between 300 and 800 nm and contained nitrate, sulfate, and organic chemicals with a noticeable degree of oxidation. The mode was generally of a larger diameter during the summer sampling period and carried more mass. The sources of the particles of this mode appeared to be located outside of the cities where they were observed. In situ processing was also observed for these particles during a period of low wind speed.

[48] **Acknowledgments.** Gas phase, National Atmospheric Emissions Inventory and Air Quality Statistics Database data were taken from of the U.K. National Air Quality Information Archive. Back trajectories were calculated by the British Atmospheric Data Centre. Coastline data used in trajectory plots were taken from of the U.S. National Geophysical Data Center. This work was funded by the U.K. Natural Environment Research Council (NERC) through research grant GR3/12499. The Edinburgh site infrastructure and MOUDI deployment and analysis were funded by the Sources And Sinks of Urban Aerosol (SASUA) project of the NERC Urban Regeneration and the Environment (URGENT) thematic program, grant GST 022244. Acknowledgement is gratefully given to Dorothy Marsh of the City of Edinburgh Council for access to the Edinburgh measurement site. James D. Allan is in receipt of a NERC studentship NER/S/A/2000/03653.

## References

- Allan, J. D., J. L. Jimenez, H. Coe, K. N. Bower, P. I. Williams, M. R. Canagaratna, J. T. Jayne, and D. R. Worsnop, Quantitative sampling using an Aerodyne aerosol mass spectrometer, 1, Techniques of data interpretation and error analysis, *J. Geophys. Res.*, **108**, 10.1029/2002JD002358, in press, 2003.
- Allen, J. O., D. P. Fergenson, E. E. Gard, L. S. Hughes, B. D. Morrical, M. J. Kleeman, D. S. Gross, M. E. Galli, K. A. Prather, and G. R. Cass, Particle detection efficiencies of aerosol time of flight mass spectrometers under ambient sampling conditions, *Environ. Sci. Technol.*, **34**(1), 211–217, 2000.
- Bower, K. N., et al., ACE-2 HILLCLOUD: An overview of the ACE-2 ground-based cloud experiment, *Tellus, Ser. B*, **52**(2), 750–778, 2000.
- Brook, R. D., J. R. Brook, B. Urch, R. Vincent, S. Rajagopalan, and F. Silverman, Inhalation of fine particulate air pollution and ozone causes acute arterial vasoconstriction in healthy adults, *Circulation*, **105**(11), 1534–1536, 2002.
- Chandler, A. S., T. W. Choularton, G. J. Dollard, M. J. Gay, M. W. Gallagher, T. A. Hill, B. M. R. Jones, S. A. Penkett, B. J. Tyler, and B. Bandy, A field-study of the oxidation of SO<sub>2</sub> in a cap cloud at Great Dun Fell, *Q. J. R. Meteorol. Soc.*, **115**(486), 397–420, 1989.
- Chow, J. C., Measurement methods to determine compliance with ambient air-quality standards for suspended particles, *J. Air Waste Manage. Assoc.*, **45**(5), 320–382, 1995.
- Cocker, D. R., N. E. Whitlock, R. C. Flagan, and J. H. Seinfeld, Hygroscopic properties of Pasadena, California aerosol, *Aerosol Sci. Technol.*, **35**(2), 637–647, 2001.
- Colville, R. N., E. J. Hutchinson, J. S. Mindell, and R. F. Warren, The transport sector as a source of air pollution, *Atmos. Environ.*, **35**(9), 1537–1565, 2001.
- Department for Environment Food and Rural Affairs, *The air quality strategy for England, Scotland, Wales and Northern Ireland, Rep. 01EP0538*, London, 2001.
- Dockery, D. W., C. A. Pope, X. P. Xu, J. D. Spengler, J. H. Ware, M. E. Fay, B. G. Ferris, and F. E. Speizer, An association between air-pollution and mortality in 6 United States cities, *New Engl. J. Med.*, **329**(24), 1753–1759, 1993.
- Dorsey, J. R., E. Nemitz, M. W. Gallagher, D. Fowler, P. I. Williams, K. N. Bower, and K. M. Beswick, Direct measurements and parameterisation of aerosol flux, concentration and emission velocity above a city, *Atmos. Environ.*, **36**(5), 791–800, 2002.
- Environmental Protection Agency, National ambient air quality standards for particulate matter; Final rule, 40 CFR part 50, *Fed. Regist.*, **62**, 138, 1997.
- Fenger, J., Urban air quality, *Atmos. Environ.*, **33**(29), 4877–4900, 1999.
- Finlayson-Pitts, B. J., and J. N. Pitts, Tropospheric air pollution: Ozone, airborne toxics, polycyclic aromatic hydrocarbons, and particles, *Science*, **276**(5315), 1045–1052, 1997.
- Harrison, R. M., and J. X. Yin, Particulate matter in the atmosphere: Which particle properties are important for its effects on health?, *Sci. Total Environ.*, **249**(1–3), 85–101, 2000.
- Jacobson, M. C., H. C. Hansson, K. J. Noone, and R. J. Charlson, Organic atmospheric aerosols: Review and state of the science, *Rev. Geophys.*, **38**(2), 267–294, 2000.
- Jayne, J. T., D. C. Leard, X. F. Zhang, P. Davidovits, K. A. Smith, C. E. Kolb, and D. R. Worsnop, Development of an aerosol mass spectrometer for size and composition analysis of submicron particles, *Aerosol Sci. Technol.*, **33**(1–2), 49–70, 2000.
- Jimenez, J. L., Jill Bauman, Philip Russell, Marvin Geller, and Patrick Hamill, Ambient aerosol sampling using the Aerodyne aerosol mass spectrometer, *J. Geophys. Res.*, **10.1029/2001JD001213**, in press, 2003.
- Kane, D. B., and M. V. Johnston, Size and composition biases on the detection of individual ultrafine particles by aerosol mass spectrometry, *Environ. Sci. Technol.*, **34**(23), 4887–4893, 2000.
- Kleeman, M. J., J. J. Schauer, and G. R. Cass, Size and composition distribution of fine particulate matter emitted from motor vehicles, *Environ. Sci. Technol.*, **34**(7), 1132–1142, 2000.
- Künzli, N., R. Kaiser, S. Medina, M. Studnicka, O. Chanel, P. Filliger, M. Herry, F. Horak, V. Puybonnieux-Texier, P. Quénel, J. Schneider, R. Seethaler, J. C. Vergnaud, and H. Sommer, Public-health impact of outdoor and traffic-related air pollution: A European assessment, *Lancet*, **356**(9232), 795–801, 2000.
- Larssen, S., R. Sluyter, and C. Helmis, Criteria for EUROAIRNET the EEA Air Quality Monitoring and Information Network, *Tech. Rep. 12*, Eur. Environ. Agency, Copenhagen, 1999.
- Liu, D. Y., D. Rutherford, M. Kinsey, and K. A. Prather, Real-time monitoring of pyrotechnically derived aerosol particles in the troposphere, *Anal. Chem.*, **69**(10), 1808–1814, 1997.
- Liu, D. Y., K. A. Prather, and S. V. Hering, Variations in the size and chemical composition of nitrate-containing particles in Riverside, CA, *Aerosol Sci. Technol.*, **33**(1–2), 71–86, 2000.
- Mayer, H., Air pollution in cities, *Atmos. Environ.*, **33**(24–25), 4029–4037, 1999.
- McLafferty, F. W., and F. Turecek, *Interpretation of Mass Spectra*, Univ. Sci., Mill Valley, Calif., 1993.
- McMurry, P. H., A review of atmospheric aerosol measurements, *Atmos. Environ.*, **34**(12–14), 1959–1999, 2000.
- McMurry, P. H., and M. R. Stolzenburg, On the sensitivity of particle-size to relative-humidity for Los-Angeles aerosols, *Atmos. Environ.*, **23**(2), 497–507, 1989.
- McMurry, P. H., M. Litchy, P. F. Huang, X. P. Cai, B. J. Turpin, W. D. Dick, and A. Hanson, Elemental composition and morphology of individual particles separated by size and hygroscopicity with the TDMA, *Atmos. Environ.*, **30**(1), 101–108, 1996.
- McMurry, P. H., X. Wang, K. Park, and K. Ehara, The relationship between mass and mobility for atmospheric particles: A new technique for measuring particle density, *Aerosol Sci. Technol.*, **36**(2), 227–238, 2002.
- Murphy, D. M., and D. S. Thomson, Laser ionization mass-spectroscopy of single aerosol-particles, *Aerosol Sci. Technol.*, **22**(3), 237–249, 1995.
- Murphy, D. M., D. S. Thomson, and T. M. J. Mahoney, In situ measurements of organics, meteoritic material, mercury, and other elements in aerosols at 5 to 19 kilometers, *Science*, **282**(5394), 1664–1669, 1998.
- Nevalainen, J., and J. Pekkanen, The effect of particulate air pollution on life expectancy, *Sci. Total Environ.*, **217**(1–2), 137–141, 1998.
- Peters, A., D. W. Dockery, J. E. Muller, and M. A. Mittleman, Increased particulate air pollution and the triggering of myocardial infarction, *Circulation*, **103**(23), 2810–2815, 2001.



- Pope, C. A., R. T. Burnett, M. J. Thun, E. E. Calle, D. Krewski, K. Ito, and G. D. Thurston, lung cancer, cardiopulmonary mortality, and long-term exposure to fine particulate air pollution, *J. Am. Med. Assoc.*, 287(9), 1132–1141, 2002.
- Prather, K. A., T. Nordmeyer, and K. Salt, Real-time characterization of individual aerosol-particles using time-of-flight mass-spectrometry, *Anal. Chem.*, 66(9), 1403–1407, 1994.
- Press, W. H., *Numerical Recipes in C: The Art of Scientific Computing*, Cambridge Univ. Press, New York, 1992.
- Ramanathan, V., P. J. Crutzen, J. T. Kiehl, and D. Rosenfeld, Atmosphere—Aerosols, climate, and the hydrological cycle, *Science*, 294(5549), 2119–2124, 2001.
- Saxena, P., and L. M. Hildemann, Water-soluble organics in atmospheric particles: A critical review of the literature and application of thermodynamics to identify candidate compounds, *J. Atmos. Chem.*, 24(1), 57–109, 1996.
- Schwartz, J., Air-pollution and daily mortality—A review and meta analysis, *Environ. Res.*, 64(1), 36–52, 1994.
- Seaton, A., W. Macnee, K. Donaldson, and D. Godden, Particulate air-pollution and acute health-effects, *Lancet*, 345(8943), 176–178, 1995.
- Seinfeld, J. H., and S. N. Pandis, *Atmospheric chemistry and physics: From air pollution to climate change*, pp. 724–7270, John Wiley, New York, 1998.
- Silva, P. J., and K. A. Prather, On-line characterization of individual particles from automobile emissions, *Environ. Sci. Technol.*, 31(11), 3074–3080, 1997.
- Silva, P. J., and K. A. Prather, Interpretation of mass spectra from organic compounds in aerosol time-of-flight mass spectrometry, *Anal. Chem.*, 72(15), 3553–3562, 2000.
- Swietlicki, E., A closure study of sub-micrometer aerosol particle hygroscopic behaviour, *Atmos. Res.*, 50(3–4), 205–240, 1999.
- Tobias, H. J., D. E. Beving, P. J. Ziemann, H. Sakurai, M. Zuk, P. H. McMurry, D. Zarling, R. Waytulonis, and D. B. Kittelson, Chemical analysis of diesel engine nanoparticles using a nano-DMA/thermal desorption particle beam mass spectrometer, *Environ. Sci. Technol.*, 35(11), 2233–2243, 2001.
- Turpin, B. J., and J. J. Huntzicker, Secondary formation of organic aerosol in the Los-Angeles basin—A descriptive analysis of organic and elemental carbon concentrations, *Atmos. Environ., Part A*, 25(2), 207–215, 1991.
- Turpin, B. J., and J. J. Huntzicker, Identification of secondary organic aerosol episodes and quantification of primary and secondary organic aerosol concentrations during scaqs, *Atmos. Environ.*, 29(23), 3527–3544, 1995.
- Turpin, B. J., P. Saxena, and E. Andrews, Measuring and simulating particulate organics in the atmosphere: Problems and prospects, *Atmos. Environ.*, 34(18), 2983–3013, 2000.
- Weingartner, E., U. Baltensperger, and H. Burtscher, Growth and structural-change of combustion aerosols at high relative-humidity, *Environ. Sci. Technol.*, 29(12), 2982–2986, 1995.
- Weingartner, E., H. Burtscher, and U. Baltensperger, Hygroscopic properties of carbon and diesel soot particles, *Atmos. Environ.*, 31(15), 2311–2327, 1997.
- Williams, P. I., M. W. Gallagher, T. W. Choularton, H. Coe, K. N. Bower, and G. McFiggans, Aerosol development and interaction in an urban plume, *Aerosol Sci. Technol.*, 32(2), 120–126, 2000.
- Zhang, X. Q., and P. H. McMurry, Theoretical-analysis of evaporative losses from impactor and filter deposits, *Atmos. Environ.*, 21(8), 1779–1789, 1987.
- Zhang, X. Q., and P. H. McMurry, Evaporative losses of fine particulate nitrates during sampling, *Atmos. Environ., Part A*, 26(18), 3305–3312, 1992.

---

M. R. Alfarra, Department of Chemical Engineering, University of Manchester Institute of Science and Technology, PO Box 88, Manchester M60 1QD, UK. (m.alfarra@student.umist.ac.uk)

J. D. Allan, K. N. Bower, H. Coe, M. W. Gallagher, and P. I. Williams, Department of Physics, University of Manchester Institute of Science and Technology, PO Box 88, Manchester M60 1QD, UK. (james.allan@physics.org; keith.bower@umist.ac.uk; hugh.coe@umist.ac.uk; martin.gallagher@umist.ac.uk; paul.i.williams@umist.ac.uk)

M. R. Canagaratna, J. T. Jayne, and D. R. Worsnop, Aerodyne Research Incorporated, 45 Manning Road, Billerica, MA 01821-3976, USA. (mrcana@aerodyne.com; jayne@aerodyne.com; worsnop@aerodyne.com)

J. L. Jimenez, Department of Chemistry and Cooperative Institute for Research in the Environmental Sciences (CIRES), University of Colorado, Boulder, CO 80309-0216, USA. (jose.jimenez@colorado.edu)

A. G. McDonald and E. Nemitz, Centre for Ecology and Hydrology Edinburgh, Bush Estate, Penicuik, Midlothian EH26 0QB, UK. (agmd@ceh.ac.uk; en@ceh.ac.uk)

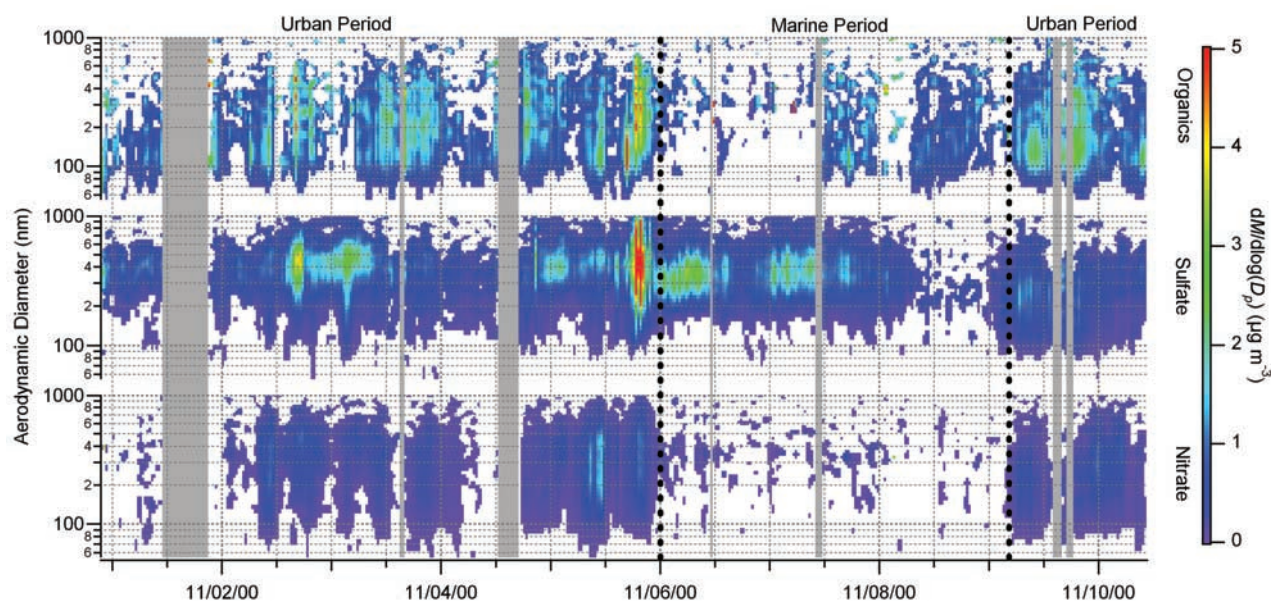


**Figure 8.** Calculated mass distributions of nitrate, sulfate, and organics from Edinburgh during November 2000. The data have been smoothed using a  $2 \times 2$  point Gaussian method, and data points below a calculated  $2\sigma$  threshold level (as described by Allan *et al.* [2003]) have been removed to improve clarity.

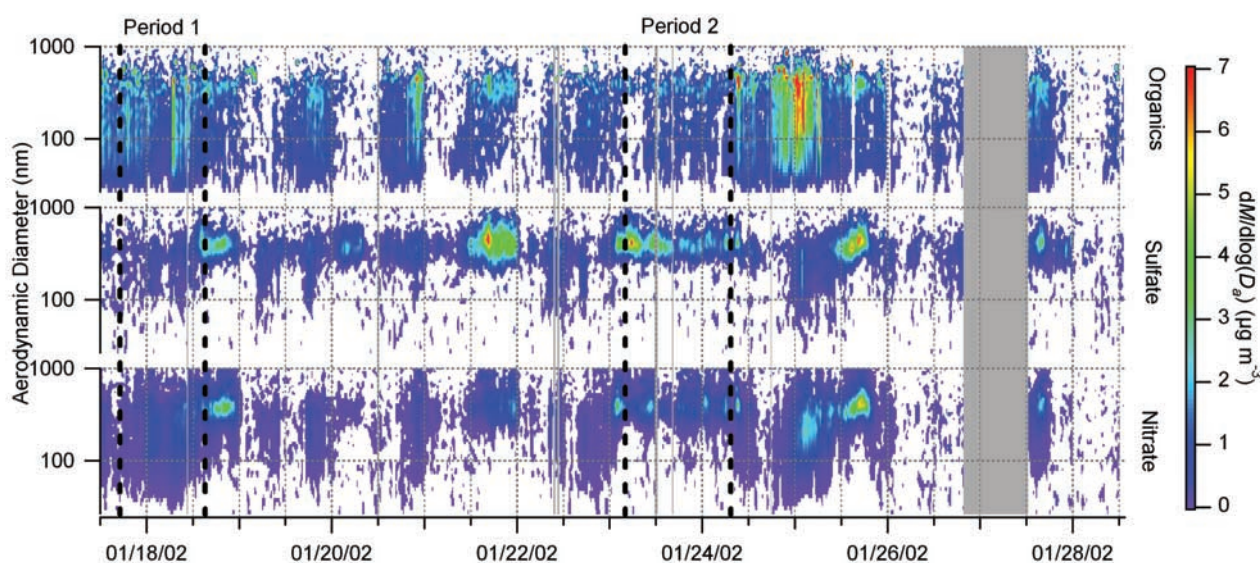


**Figure 12.** Calculated mass distributions from Manchester for January 2002. A smoothing and filtering process identical to that used for the Edinburgh data has been applied.

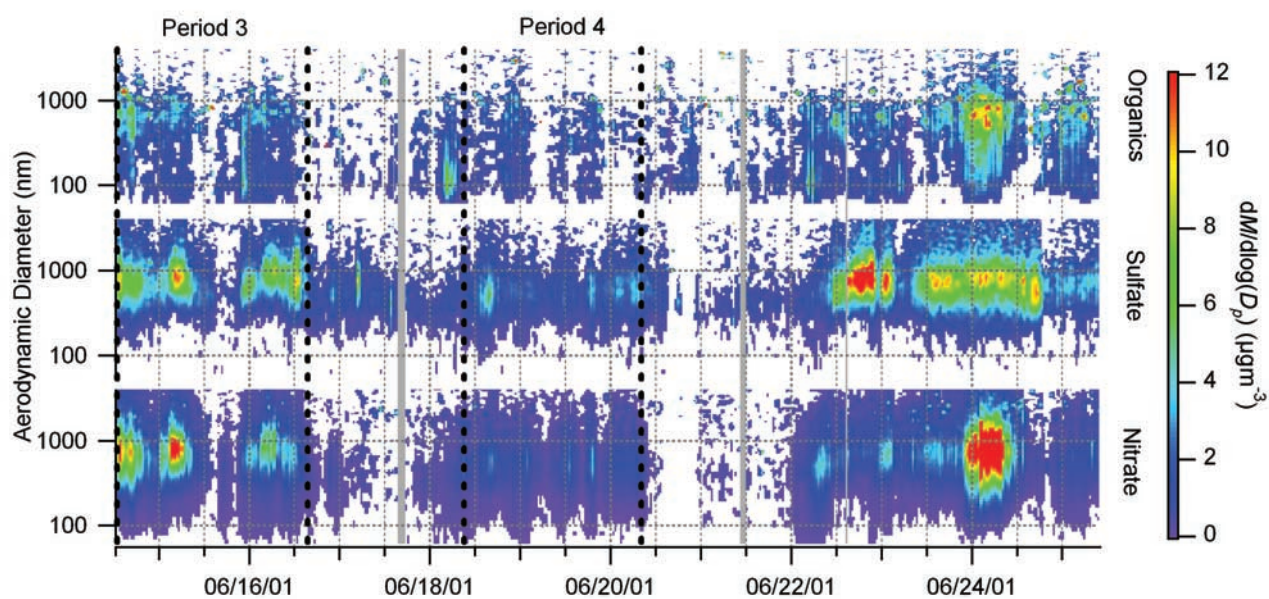


**Figure 16.** Calculated mass distributions from Manchester for June 2001. The same smoothing and filtering process has been applied as previously.